Volume 24, No 4 | International Journal of Radiation Research, October 2026

Treatment of high-altitude polycythemia with radiopharmaceutical platform of poly (lactic-co-glycolic acid) nanoparticles loaded with hydroxyurea

J. Nie[1*], D. Wang[2], M.J. Li[3]

[1]*School of Ethnic Medicine, Chengdu University of Traditional Chinese Medicine, Chengdu, China*
[2]*School of Pharmacy, Chengdu University of Traditional Chinese Medicine, Chengdu, China*
[3]*College of Medical Technology, Chengdu University of Traditional Chinese Medicine, Chengdu, China*

► ***Original article***

Corresponding author:
Jia Nie, Ph.D.,
E-mail: *fcmlnj@163.com*

Received: November 2025
Final revised: March 2026
Accepted: April 2026

Int. J. Radiat. Res., October 2026; 24(4): 1007-1015

DOI: 10.61186/ijrr.24.4.10

Keywords: *Hydroxyurea, PLGA nanoparticles, radiopharmaceutical platform, technetium-99m, high altitude polycythemia, biodistribution, liver function, coagulation indices.*

ABSTRACT

Background: High Altitude Polycythemia (HAPC) is a chronic hypoxia-related disorder characterized by excessive erythrocytosis, hypercoagulability, and organ dysfunction. Hydroxyurea (HU) is used clinically but is limited by systemic toxicity and suboptimal targeting. This study aimed to evaluate the therapeutic efficacy and biodistribution of a radiopharmaceutical platform based on poly(lactic-co-glycolic acid) nanoparticles loaded with hydroxyurea (HU-PLGA-NPs) in an experimental HAPC model. ***Materials and Methods:*** Sixty male Sprague–Dawley rats with hypobaric hypoxia-induced HAPC were randomized into three groups: HU-PLGA-NPs, conventional HU, and supportive treatment. Nanoparticles were radiolabeled with technetium-99m to assess in vivo biodistribution using SPECT/CT imaging. Hematological parameters, coagulation indices, hemorheology, immune markers, bone marrow apoptosis, and liver and renal function were evaluated over 12 weeks. ***Results:*** HU-PLGA-NP treatment significantly reduced hemoglobin, hematocrit, blood viscosity, and coagulation abnormalities compared with conventional HU and supportive therapy ($p<0.05$). Imaging and biodistribution studies demonstrated preferential accumulation in bone marrow and spleen. Improved immune parameters and reduced hepatic and renal toxicity were observed in the nanoparticle group. ***Conclusions:*** The HU-PLGA-NP radiopharmaceutical platform enhances therapeutic efficacy and targeting while reducing systemic toxicity in HAPC, representing a promising strategy for precision treatment.

INTRODUCTION

High Altitude Polycythemia (HAPC) is a chronic hypoxia-induced disorder that poses a major health threat to long-term residents of high-altitude regions [1, 2]. Persistent hypoxic stimulation drives excessive erythropoiesis, resulting in markedly elevated hemoglobin (Hb) levels, increased hematocrit (Hct), and drastically increased blood viscosity [3, 4]. These changes impair microcirculation, aggravate tissue oxygen deficiency, and significantly elevate the risk of thrombotic events, cardiovascular and cerebrovascular complications, and progressive hepatic and renal dysfunction [5-7].

Hydroxyurea remains the most commonly used pharmacologic option for HAPC, but it exhibits several important clinical limitations [8]. Its non-targeted systemic distribution results in low effective drug concentration at the bone marrow where abnormal erythropoiesis originates necessitating higher doses and prolonged treatment courses [9]. This contributes to poor patient compliance and increases the likelihood of systemic toxicities including bone marrow suppression (BMS), hepatotoxicity, gastrointestinal symptoms, and secondary metabolic disturbances [10]. Critically, conventional hydroxyurea administration cannot selectively regulate pathological hematopoietic stem/progenitor cells, thereby limiting its ability to fundamentally correct the dysregulated erythropoietic process.

Poly(lactic-co-glycolic acid) (PLGA), a biodegradable and biocompatible polymer approved by the FDA, offers a promising solution for targeted drug delivery [11]. PLGA nanoparticles (NPs) in the 100–200 nm range exhibit prolonged circulation and passive targeting toward highly perfused and metabolically active tissues such as bone marrow through enhanced permeability and retention effects [12, 13]. HU-loaded PLGA nanoparticles (HU-PLGA-NPs) can thus enhance local drug bioavailability, achieve controlled release, and reduce systemic exposure, providing a more efficient and safer therapeutic strategy for HAPC than free hydroxyurea [14].

Despite these advantages, one major limitation persists: the inability to directly visualize and quantitatively evaluate nanoparticle biodistribution in vivo, which is essential for validating bone marrow

[Downloaded from mail.ijrr.com on 2026-11-11]

[DOI: 10.61186/ijrr.24.4.10]

targeting, optimizing dosage, ensuring safety, and understanding therapeutic mechanisms [15]. To address this challenge, radiopharmaceutical technologies offer a unique opportunity [16]. Radiolabeling nanoparticles with gamma- or positron -emitting isotopes enables real-time tracking through SPECT or PET imaging, allowing precise visualization of their organ distribution, bone marrow uptake, pharmacokinetics, and clearance pathways [15].

Radiopharmaceutical nanoplatforms thus integrate therapy and diagnostic imaging (nanotheranostics), improving treatment precision and enabling individualized dose optimization [17]. Incorporating a radiolabeled tracer such as technetium-99m (^{99m}Tc) into HU-PLGA-NPs transforms the system into a dual-function platform capable of both targeted drug delivery and non-invasive imaging guidance [22]. Such an approach is particularly valuable for HAPC, where confirming selective bone marrow uptake is critical for disease correction and long-term safety.

Based on this rationale, the present study constructs a radiopharmaceutical PLGA nanoparticle platform loaded with hydroxyurea (^{99m}Tc-HU-PLGA-NPs) aimed at achieving precise bone marrow-targeted therapy for HAPC while simultaneously enabling real-time biodistribution imaging. By leveraging the synergistic effects of PLGA-based controlled release, radiotracer-guided targeting, and hydroxyurea's therapeutic activity, this strategy is designed to enhance therapeutic efficacy, reduce systemic toxicity, shorten treatment duration, and provide mechanistic insight through molecular imaging. This study evaluates the physicochemical characteristics, radiolabeling stability, biodistribution patterns, therapeutic performance, and safety profile of the proposed nanotheranostic platform in a rat model of HAPC.

MATERIALS AND METHODS

Research subject

A total of 60 healthy adult male Sprague–Dawley (SD) rats, weighing 180–220 g, were used in this study. All rats were housed under standard laboratory conditions at a room temperature of 22 ± 2 °C and relative humidity of 50 ± 10%, with a 12/12 h light–dark cycle and free access to food and water. Animals were allowed to acclimatize for 1 week prior to any experimental procedure [3].

After successful establishment of the HAPC model, rats were randomly allocated using a random number table into three groups (n=20 per group):

Experimental Group (EG): treated with radiolabeled hydroxyurea-loaded PLGA nanoparticles (^{99m}Tc-HU-PLGA-NPs);

Control Group (CG): treated with conventional hydroxyurea;

Observation Group (OG): received general supportive therapy.

A subset of rats in the EG and CG (n=6 per group) was additionally used for radiopharmaceutical imaging and ex vivo biodistribution analysis.

All experimental procedures were reviewed and approved by the Ethical Committee of the School of Ethnic Medicine, Chengdu University of Traditional Chinese Medicine, and conducted in accordance with institutional and national guidelines for the care and use of laboratory animals.

Inclusion criteria

Rats were included if they successfully established the HAPC model, evidenced by four consecutive weeks of simulated 5,000 m hypoxic exposure (≈ 54 kPa; ≈ 11.0% O_2 partial pressure), achieving post-modeling hemoglobin (Hb) levels ≥ 200 g/L and hematocrit (Hct) ≥ 65% [4, 5], and exhibiting typical hypoxia manifestations such as decreased activity, piloerection, reduced fur glossiness, and dark red mucosal discoloration. General health status required normal baseline body weight, food intake (FI), water intake (WI), and activity, with no signs of systemic disease prior to modeling and no concurrent administration of drugs affecting hematopoiesis, coagulation, or hemorheology during the experiment. Blood samples for analysis were required to be free from hemolysis or clotting, obtained smoothly via repeated tail vein sampling, and fully meeting analytical requirements [6, 7]. Finally, all procedures had to comply with ethical standards, with approval from the Animal Ethics Review Committee (AERC) and strict adherence to the "3R" principle.

Exclusion criteria

Rats were excluded if they presented with spontaneous tumors, severe infections, or other serious systemic diseases prior to or during the experiment. Exclusion also applied to animals failing to meet HAPC modeling criteria (Hb<200 g/L and/or Hct<65%) after hypoxic exposure, or those experiencing accidental death during modeling or drug administration (e.g., anesthesia or gavage errors). Animals reaching a humane endpoint due to marked deterioration of general condition from experimental procedures, defined as >20% body weight loss from baseline or severe lethargy [8, 9], were also excluded. Furthermore, rats with severe hemolysis, clotting, or contamination of blood samples precluding accurate testing, or those with major deviations in drug dose or frequency due to operational errors, were excluded. Finally, severe acute allergic reactions or intolerance to hydroxyurea, PLGA nanoparticles, or radiolabeled formulations, such as severe seizures, intractable diarrhea leading to dehydration, or life-threatening reactions, resulted in exclusion.

[Downloaded from mail.ijrr.com on 2026-11-11]

[DOI: 10.61186/ijrr.24.4.10]

TREATMENT

Control Group (CG)

Rats received conventional hydroxyurea therapy. Commercial tablets (Hengrui Pharmaceutical Co., Ltd., China; NMPA No. H32023112) were dissolved in sterile saline and administered by oral gavage. An initial dose of 20 mg/kg/day was given, followed by a maintenance dose of 10–15 mg/kg/day after one week based on serial complete blood counts [10–13].

Routine hematologic monitoring (RBC, Hb, Hct) was performed weekly. When indices remained above the HAPC thresholds (Hb≥200 g/L or Hct≥65%) without significant decline, small-volume phlebotomy was applied as needed.

Experimental Group (EG)

Rats received ^{99m}Tc-HU-PLGA nanoparticles. HU-PLGA-NPs were synthesized by emulsion solvent evaporation (encapsulation efficiency >80%, drug loading >10%, particle size 100–200 nm). Nanoparticles were subsequently radiolabeled with ^99mTc using an appropriate reducing and chelating system, achieving high radiochemical purity.

Therapy consisted of tail-vein injections of ^{99m}Tc-HU-PLGA-NPs at a hydroxyurea-equivalent dose of 20 mg/kg twice weekly for 12 weeks. Radioactivity per dose was optimized for imaging while remaining within safe exposure limits. Hematologic indices and liver/kidney function were monitored to assess potential drug- and radiation-related toxicity [14–16].

A subset of rats (n = 6) underwent serial SPECT/CT imaging and ex vivo biodistribution to evaluate in vivo targeting and pharmacokinetics.

Observation Group (OG)

Rats received supportive care consisting of intraperitoneal glutathione for hepatoprotection and intermittent low-flow oxygen therapy. Monitoring included complete blood count, oxygen saturation, and serum uric acid.

Across all groups, small-volume phlebotomy was permitted if Hct exceeded 70%. Animals developing severe bone marrow suppression or serious hypersensitivity reactions were withdrawn.

Block randomization was used for group allocation. Outcome assessors were blinded to CG and EG assignments; OG was unblinded due to distinct treatment characteristics. All procedures were approved by the institutional AERC.

Evaluation metric

Evaluation of therapeutic outcomes included coagulation function, hematologic response, hemorheology, bone marrow apoptosis, organ toxicity, and radiopharmaceutical biodistribution. Tail-vein blood was collected at baseline and at 3, 6, and 12 weeks to measure PT, APTT, fibrinogen, and D-dimer using an automated coagulation analyzer, allowing assessment of treatment-related changes in hypercoagulability [17, 18]. Therapeutic efficacy was classified as significant (Hb ≤ 180 g/L with symptom resolution), effective (Hb decrease ≥ 20 g/L with notable symptom improvement), or invalid (failure to meet these criteria or clinical deterioration). The overall effective rate was calculated as (significant + effective)/total × 100 to compare the regulatory impact of each regimen on Hb levels and HAPC symptoms [19, 20]. Hemorheological parameters - including whole blood viscosity, erythrocyte aggregation index, and erythrocyte deformation index - were obtained before treatment and at week 12 to evaluate improvements in blood flow abnormalities, particularly those targeted by the nanoparticle formulation. Complete blood counts were performed at all time points to monitor RBC indices (RBC count, Hb, Hct, reticulocyte percentage) and inflammatory markers (WBC count, neutrophil-to-lymphocyte ratio), providing a quantitative basis for assessing suppression of excessive erythropoiesis and systemic inflammation by HU-PLGA-NPs [21–23]. At 12 weeks, femoral bone marrow mononuclear cells were isolated and apoptosis was quantified using Annexin V/PI flow cytometry to determine the selective pro-apoptotic effect of the nanoparticle therapy on abnormal hematopoietic progenitors. For toxicity assessment, liver, spleen, and kidneys were weighed to calculate organ coefficients (organ weight/body weight × 100%), and tissues were processed for H&E staining to evaluate structural alterations. In the imaging subset of the experimental group, SPECT/CT scans were performed after ^{99m}mTc-HU-PLGA-NP injection, with regions of interest drawn over major organs to quantify uptake as %ID/g or standardized uptake values. *Ex vivo* biodistribution was measured using a gamma counter. These imaging and biodistribution data were used to characterize *in vivo* targeting, pharmacokinetics, off-target accumulation, and their correlation with hematologic and clinical outcomes.

Safety indicators

Safety was evaluated through daily monitoring of general condition (behavior, activity, intake, body weight), organ function tests (hepatic, renal, cardiac markers measured at baseline, 3, 6, and 12 weeks), histopathology of major organs, and systematic recording of all adverse events. This comprehensive approach aimed to identify any potential toxicity from repeated administration of HU PLGA nanoparticles, their radiolabeled formulation, or associated low-dose radiation exposure, including assessment of PLGA metabolite accumulation and radiopharmaceutical involvement.

Preparation of HU-PLGA nanoparticles and radiolabeling

HU-PLGA nanoparticles were prepared using a

[Downloaded from mail.ijrr.com on 2026-11-11]

[DOI: 10.61186/ijrr.24.4.10]

classical emulsion–solvent evaporation technique. Briefly, hydroxyurea and PLGA were co-dissolved in dichloromethane to obtain a homogeneous organic phase, in which the mass fraction of hydroxyurea was controlled at 10–20% (w/w) and the concentration of PLGA at 2–5% (w/v). This organic phase was slowly added to an aqueous phase containing 1% polyvinyl alcohol (PVA) under continuous probe ultrasonication, leading to the formation of an oil-in-water emulsion. The emulsion was stirred magnetically for several hours to remove the organic solvent and allow the nanoparticles to solidify. The suspension was then centrifuged at high speed to remove free drug and excess PVA, and the resulting pellet was washed repeatedly with ultrapure water. After filtration through a 0.22 μm membrane, mannitol (5%) was added as a lyoprotectant, and the preparation was freeze-dried at −50 °C for 24 hours to obtain a loose white nanoparticle powder. The particle size was subsequently adjusted to approximately 100–200 nm by fine-tuning sonication conditions, and the nanoparticles were stored at 4 °C to minimize PLGA hydrolysis.

To construct the radiopharmaceutical platform, HU-PLGA nanoparticles were further radiolabeled with technetium-99m (^{99m}Tc). For this purpose, a defined amount of the lyophilized nanoparticles was resuspended in nitrogen-purged saline, and a freshly prepared stannous chloride solution was added as a reducing agent. Freshly eluted $^{99m}TcO_4^-$ was then introduced into the suspension, and the mixture was incubated at room temperature for approximately 15 –20 minutes to allow ^{99m}Tc to bind to the nanoparticle surface. Radiochemical purity was assessed using instant thin-layer chromatography with appropriate mobile phases, and only preparations with radiochemical purity above 95% were used for *in vivo* experiments. The stability of the radiolabeled formulation was evaluated by incubating ^{99m}Tc-HU-PLGA nanoparticles in serum at different time points and re-assessing radiochemical purity. Throughout the process, we ensured that radiolabeling did not significantly alter the particle size distribution or compromise the encapsulation characteristics of the HU-PLGA nanoparticles.

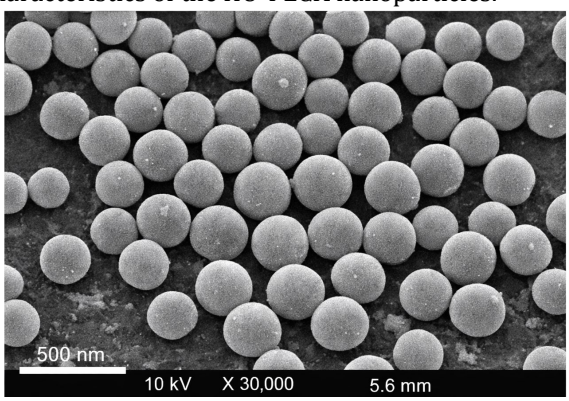


Figure 1. Scanning electron micrograph of hydroxyurea-loaded PLGA nanoparticles.

Euthanasia procedure

At the conclusion of the experimental period or upon reaching humane endpoints, rats were euthanized according to animal welfare regulations using intraperitoneal injection of pentobarbital sodium (150 mg/kg; 60 mg/mL in physiological saline). Anesthesia was induced within 1–2 minutes, followed by death via respiratory depression. Confirmation of death was based on persistent pupillary dilation with absent light and corneal reflexes, and cessation of heartbeat and spontaneous breathing for over 3 minutes. Immediately following confirmation, thoracic and abdominal cavities were opened. Samples of liver, kidney, spleen, heart, and bone marrow were collected for subsequent biochemical, histopathological, and, in the radiopharmaceutical group, ex vivo biodistribution analyses. All carcasses and biological waste, including radioactive materials, were disposed of as medical and low-level radioactive waste by qualified institutions.

Statistical methods

Data were analyzed using SPSS V.23. Continuous variables were assessed for normality using the Shapiro–Wilk test. Normally distributed data were analyzed using repeated-measures ANOVA to compare changes in hemoglobin, hematocrit, and coagulation parameters across groups over time. Non -normally distributed data were analyzed using the Kruskal–Wallis test. Categorical variables, such as overall treatment response rates, were compared using the chi-square or Fisher's exact test, with the Cochran–Mantel–Haenszel test used to control for stratification factors. Bonferroni correction was applied for multiple pairwise comparisons. Missing data were handled through exclusion or multiple imputation, depending on their proportion and distribution.

For radiopharmaceutical biodistribution, organ uptake (%ID/g) was analyzed using one-way ANOVA or non-parametric equivalents. Correlations between bone marrow uptake and hematologic improvement were assessed via Pearson or Spearman coefficients, based on data distribution. All analyses were performed using SPSS 26.0 and R 4.2.1, with statistical significance defined as a two-sided p value ≤ 0.05.

RESULTS

Comparison of general information for different groups

Before treatment, the three groups of rats showed comparable baseline characteristics. As shown in Table 1, there were no statistically significant differences among the CG, EG, and OG in body weight, hemoglobin level before modeling, hemoglobin and

[Downloaded from mail.ijrr.com on 2026-11-11]

[DOI: 10.61186/ijrr.24.4.10]

hematocrit after modeling, food intake (FI), or water intake (WI) (all p>0.05) (table 1). All animals successfully met the diagnostic criteria for HAPC after low-pressure hypoxic exposure (Hb ≥ 200 g/L and Hct ≥ 65%), resulting in a 100% modeling success rate in each group.

These findings indicate that the general condition and model severity of HAPC were well balanced among the three groups before the initiation of different treatments, providing a reliable foundation for subsequent comparisons of therapeutic efficacy.

Table 1. Comparison of general baseline data of three groups of rats.

Parameter	CG (n = 20)	EG (n = 20)	OG (n = 20)	p
Body Weight (g, mean ± SD)	205.5±10.8	208.2±11.5	203.7±9.6	0.487
Hb before modeling (g/L, mean ± SD)	152.3±8.5	150.8±9.1	154.1±7.9	0.522
Hb after modeling (g/L, mean ± SD)	218.5±12.5	221.3±11.8	215.9±13.1	0.405
Hct after modeling (%, mean ± SD)	68.5±3.8	69.2±4.1	67.8±3.5	0.536
Successfully modeled (n, %)	20 (100%)	20 (100%)	20 (100%)	1.000
FI (g/day, mean ± SD)	25.3±2.1	24.8±2.4	25.6±1.9	0.532
WI (mL/day, mean ± SD)	35.6±3.2	34.9±3.5	36.1±2.8	0.491

Note: Hb: Hemoglobin, Hct: Hematocrit, FI: Food intake, WI: water intake.

Comparison of coagulation function indicators after 3 weeks of treatment

After 3 weeks of treatment, coagulation function began to diverge among the three groups. Rats in the experimental group (EG), treated with HU-PLGA nanoparticle–based therapy, showed significantly shorter PT and APTT values compared with the control group (CG) and observation group (OG) (p<0.05) (table 2).

At the same time, fibrinogen (FIB) and D-dimer levels in the EG were markedly lower than those in the CG and OG (p<0.05), indicating an early and meaningful improvement of the hypercoagulable state. These results suggest that, even in the initial treatment phase, the nanoparticle-based regimen is more effective than conventional hydroxyurea and supportive therapy in reducing thrombotic risk in HAPC rats.

Table 2. Coagulation indicators of rats in different groups after 3 weeks of treatment.

Parameter	CG (n = 20)	EG (n = 20)	OG (n = 20)	Inter-group p	EG vs CG (p)
PT (s)	15.8±1.6	13.2±1.1 **	15.6±1.4	0.016	0.013
APTT (s)	28.5±3.2	22.3±2.5 **	27.9±2.9	0.023	0.018
FIB (g/L)	3.2±0.5	2.1±0.3 **	3.1±0.4	0.019	0.015
D-Dimer (μg/mL)	2.5±0.6	1.2±0.3 **	2.4±0.5	0.027	0.022

Note: ** indicates comparison with CG, p<0.05. PT: prothrombin time, APTT: activated partial thromboplastin time, FIB: fibrinogen.

Comparison of coagulation function indicators after 6 weeks of treatment

By week 6, the differences in coagulation function among the three groups had become more pronounced. The EG maintained significantly shorter PT and APTT values than both the CG and OG (inter-group p<0.01), indicating further normalization of coagulation times (table 3).

Fibrinogen levels in the EG had decreased to 1.9 ± 0.3 g/L, significantly lower than those in the CG and OG, and D-dimer values dropped to 0.8 ± 0.2 μg/mL, the lowest among all groups (p<0.01 for EG vs CG) (table 3). The CG exhibited partial improvement compared with baseline, but remained clearly inferior to the EG, while the OG showed only limited change. These findings demonstrate that the nanoparticle-based treatment provides a faster and more robust correction of hypercoagulability than conventional hydroxyurea or supportive therapy alone.

Table 3. Coagulation indicators of rats in different groups after 6 weeks of treatment.

Parameter	CG (n = 20)	EG (n = 20)	OG (n = 20)	Inter-group p	EG vs CG (p)
PT (s)	16.2±1.4	12.5±1.0 **	15.9±1.3	0.005	0.003
APTT (s)	29.8±3.1	21.6±2.2 **	28.5±2.8	0.006	0.002
FIB (g/L)	3.5±0.5	1.9±0.3 **	3.3±0.4	0.007	0.004
D-Dimer (μg/mL)	2.8±0.5	0.8±0.2 **	2.6±0.4	0.004	0.001

Note: ** indicates comparison with CG, p < 0.05. PT: prothrombin time, APTT: activated partial thromboplastin time, FIB: fibrinogen.

Comparison of coagulation function indicators after 12 weeks of treatment

After 12 weeks of treatment, all groups showed some improvement in coagulation parameters compared with their pre-treatment status, but the extent of improvement varied considerably. As detailed in Table 4, rats in the EG achieved the most favorable coagulation profile.

The PT and APTT values in the EG (13.8 ± 0.9 s and 23.4 ± 2.0 s, respectively) were significantly better than those in both CG and OG (p<0.01) and were close to the normal range of healthy rats. Similarly, FIB and D-dimer levels in the EG (2.3 ± 0.3 g/L and 1.1 ± 0.2 μg/mL, respectively) were significantly lower than in the other two groups (p<0.01), indicating a stable correction of the hypercoagulable state (table 4).

In comparison, the CG showed moderate but incomplete improvement, and the OG remained the least improved. Overall, these results highlight that long-term treatment with the HU-PLGA nanoparticle-based regimen offers the most comprehensive and sustained normalization of coagulation function in HAPC model rats.

Table 4. Coagulation indicators of rats in different groups after 12 weeks of treatment.

Parameter	CG (n = 20)	EG (n = 20)	OG (n = 20)	Inter-group p	EG vs CG (p)
PT (s)	15.2±1.1	13.8±0.9 **	14.9±1.0	<0.01	<0.01
APTT (s)	27.6±2.5	23.4±2.0 **	26.8±2.3	<0.01	<0.01
FIB (g/L)	3.1±0.4	2.3±0.3 **	3.0±0.4	<0.01	<0.01
D-Dimer (μg/mL)	2.2±0.4	1.1±0.2 **	2.0±0.3	<0.01	<0.01

Note: ** indicates comparison with CG, p < 0.05. PT: prothrombin time, APTT: activated partial thromboplastin time, FIB: fibrinogen.

[Downloaded from mail.ijrr.com on 2026-11-11]

[DOI: 10.61186/ijrr.24.4.10]

Comparison of hematological indicators across treatment cycles

Figure 2 illustrates the dynamic changes in hematological parameters among the three groups over the 12-week treatment period. Across all time points, rats in the Experimental Group (EG) exhibited a sustained and marked decline in hemoglobin (Hb) levels compared with the Control Group (CG), with statistically significant differences beginning at week 3 and persisting through week 12 ($p<0.05$).

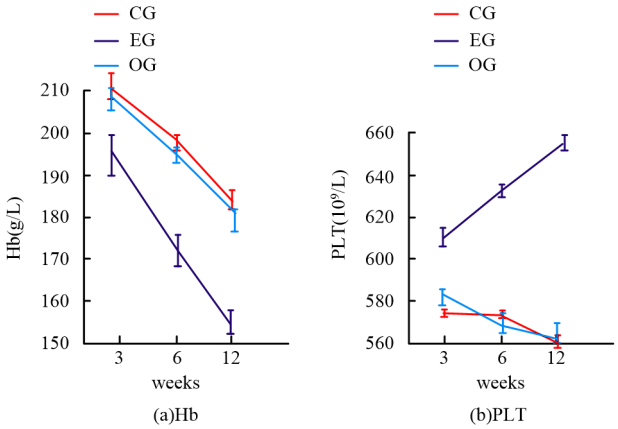


Figure 2. Changes in hematological indicators of three groups of rats at different treatment cycles.

By the end of the study, Hb levels in the EG had decreased to 152.8 ± 8.3 g/L, approaching the normal physiological range of healthy rats. In contrast, Hb in the CG remained markedly elevated at 185.4 ± 9.8 g/L, indicating insufficient therapeutic control with conventional hydroxyurea.

Platelet count (PLT) also showed a favorable upward trend in the EG, increasing from 612.5 ± 48.3 × 10^9/L at week 3 to 658.4 ± 54.7 × 10^9/L at week 12. At both weeks 6 and 12, PLT values in the EG were significantly higher than in the CG ($p<0.05$), reflecting improved bone marrow recovery and hematopoietic regulation.

Overall, the radiopharmaceutical HU-PLGA nanoparticle platform demonstrated a more pronounced normalization of hematological profiles than traditional therapy, underscoring its enhanced therapeutic effect.

Comparison of complement immune protein levels

Complement levels in the EG rose steadily throughout the study, whereas improvements in the CG and OG were slower and remained near the low-normal range.

At week 3, C3 levels in the EG were already significantly higher than those in the CG ($p<0.05$). By week 6, C3 levels in the EG (0.98 ± 0.08 g/L) approached the lower limit of the normal range for SD rats (0.9–1.8 g/L), while CG and OG remained below normal.

By week 12, both complement C3 (1.15 ± 0.07 g/L) and complement C4 (0.33 ± 0.03 g/L) in the EG had fully returned to normal values and were significantly higher than in the CG and OG ($p<0.01$).

These results suggest that HU-PLGA-NPs effectively restore immune balance and complement function more rapidly and consistently than traditional therapy.

Comparison of immunoglobulin levels among groups

At week 3, IgG concentrations in the EG had already risen above those in the CG ($p<0.05$). This upward trend continued steadily, with IgG reaching 18.5 ± 3.2 mg/mL and IgA reaching 435 ± 65 μg/mL by week 12- both significantly higher than the CG ($p<0.01$) (table 5).

In contrast, the CG and OG showed only modest increases, indicating partial but limited restoration of humoral immunity.

These findings demonstrate that HU-PLGA-NPs significantly enhance immune regulation and promote recovery of immunoglobulin production more effectively than conventional hydroxyurea.

Table 5. Comparison of immunoglobulin levels among groups.

Parameter	Group	Baseline	3 Weeks	6 Weeks	12 Weeks	Inter-group p
IgG (mg/mL)	EG	10.5±2.1	12.8±2.5 **	15.2±2.8 **	18.5±3.2 **	<0.01
	CG	10.8±2.3	11.2±2.4	12.5±2.6	13.8±2.9	
	OG	10.6±2.2	11.5±2.3	13.1±2.5	14.2±2.7	
IgA (μg/mL)	EG	285±45	325±52 **	380±58 **	435±65 **	<0.01
	CG	278±48	290±50	305±55	325±60	
	OG	280±46	295±51	315±56	345±62	

Note: ** $p < 0.01$ vs. CG. EG: Experimental group, CG: Control group, OG: Observational group.

Comparison of RBC counts and related hematological parameters

At week 3, rats in the EG already showed significantly lower RBC count, Hb, and Hct compared with the CG ($p < 0.05$). By week 6, these indicators had moved further toward normal physiological ranges.

By week 12, all major hematological indices in the EG had normalized:

RBC count: 5.72 ± 0.31 × 10^{12}/L

Hemoglobin: 156.8 ± 8.5 g/L

Hematocrit: 48.9 ± 2.8%

Reticulocytes: 2.1 ± 0.5%

These values fall within or near normal SD rat ranges, indicating a strong inhibitory effect of HU-PLGA-NPs on excessive erythropoiesis.

In contrast, both the CG and OG showed slower improvement, and their RBC and Hb levels remained above normal at week 12. Inter-group analysis showed highly significant differences ($p<0.01$) between EG and CG at every time point (table 6).

Blood rheological index (BRI) levels in the three groups

Blood rheology was significantly impaired in all groups prior to treatment, with elevated whole blood

[Downloaded from mail.ijrr.com on 2026-11-11]

[DOI: 10.61186/ijrr.24.4.10]

viscosity (WBV), increased erythrocyte aggregation index (EAI), and reduced erythrocyte deformation index (EDI). There were no significant differences among the three groups at baseline ($p>0.05$).

Table 6. Comparison of RBC counts and related indicators.

Parameter	Group	3 Weeks	6 Weeks	12 Weeks	Inter-group p	EG vs CG (p)
RBC ($\times10^{12}$/L)	EG	7.15± 0.42**	6.38± 0.36**	5.72± 0.31**	<0.01	<0.01
	CG	7.68± 0.51	7.28± 0.47	6.95± 0.43		
	OG	7.59± 0.48	7.18± 0.45	6.82±0.40		
Hemoglobin (g/L)	EG	198.5± 11.2**	175.6± 9.8 **	156.8± 8.5**	<0.01	<0.01
	CG	210.8± 12.5	200.7± 11.6	188.4± 10.8		
	OG	208.7± 12.1	198.2± 11.3	185.6± 10.5		
Hematocrit (%)	EG	62.8± 3.5**	56.3± 3.1**	48.9± 2.8**	<0.01	<0.01
	CG	67.2±4.2	63.8±3.9	59.4±3.6		
	OG	66.5±4.0	62.9±3.8	58.1±3.5		
Reticulocyte (%)	EG	4.8± 0.9**	3.2± 0.7**	2.1± 0.5**	<0.01	<0.01
	CG	6.2±1.2	5.8±1.1	5.3±1.0		
	OG	6.0±1.1	5.6±1.0	5.1±0.9		

Note: ** $p < 0.05$ vs. CG. RBC: Red blood cell.

After 12 weeks of treatment, the Experimental Group (EG) exhibited the most pronounced improvement. WBV decreased markedly from 5.85 ± 0.62 mPa·s to 3.12 ± 0.38 mPa·s, returning squarely into the normal reference range of healthy SD rats (3.0–4.5 mPa·s). Similarly, EAI improved from 7.25 ± 0.85 to 4.32 ± 0.56, and EDI increased from 0.42 ± 0.05 to 0.58 ± 0.06, both reflecting normalization of blood fluidity and red cell deformability.

Improvements in CG and OG were present but modest. WBV, EAI, and EDI in these groups remained at borderline-abnormal levels, significantly worse than the EG ($p<0.01$).

These findings indicate that the radiopharmaceutical HU-PLGA nanoparticle platform not only corrects hematological parameters but also markedly enhances hemorheology, reducing blood viscosity and improving microcirculatory flow in HAPC model rats.

Comparison of blood parameters across groups

Blood count indicators improved to different degrees across the treatment groups. The EG demonstrated the most substantial improvement after 12 weeks.

RBC count fell from 7.82 ± 0.58 × 10^{12}/L to 5.65 ± 0.42 × 10^{12}/L, hemoglobin decreased from 219 ± 16 g/L to 142 ± 11 g/L, and hematocrit dropped from 68.2 ± 4.3% to 47.8 ± 3.2%, all fully returning to normal physiological ranges for SD rats. Reticulocyte percentage also decreased from 5.2 ± 1.1% to 2.3 ± 0.6%, indicating effective suppression of excessive erythropoiesis—an essential therapeutic goal in HAPC.

In contrast, both CG and OG showed only partial improvements, and many parameters in these groups remained above normal limits. The radiopharmaceutical HU-PLGA nanoparticle therapy thus provided the strongest correction of erythroid overproduction.

Apoptosis of bone marrow mononuclear cells (BMMCs)

The apoptosis rate of bone marrow mononuclear cells increased progressively in all groups during treatment, but the magnitude was greatest in the EG. Apoptosis in the EG rose from nearly normal baseline levels (~16%) to 35.68 ± 6.92% at week 6, and further to 52.45 ± 10.38% at week 12.

This level of apoptosis indicates a robust therapeutic effect of the HU-PLGA nanoparticle formulation in promoting the selective elimination of pathological erythroid precursors-central to controlling polycythemia.

CG and OG showed smaller increases (35.83% and 45.76% respectively at week 12), demonstrating significantly weaker induction of therapeutic apoptosis compared to the EG ($p<0.05$).

Changes in liver function indicators (LFI)

Liver function was impaired in all groups prior to treatment. By week 12, the EG displayed the most significant improvements in ALT, AST, TBIL, and ALB, all of which returned to normal healthy ranges.

ALT fell from 68.2 ± 12.1 U/L to 25.8 ± 4.7 U/L, AST from 62.8 ± 10.9 U/L to 23.2 ± 4.3 U/L, and TBIL decreased to 10.5 ± 1.9 μmol/L. Albumin increased steadily to 43.8 ± 4.2 g/L.

CG showed moderate improvement, while OG demonstrated minimal recovery, indicating persistent hepatic stress under supportive therapy alone.

The EG's superior results indicate that HU-PLGA-NPs not only treat polycythemia but also protect hepatic tissue-likely due to reduced systemic hydroxyurea exposure and improved drug targeting.

Changes in renal function indicators (RFI)

Renal function was compromised in all groups before treatment. By 12 weeks, rats in the EG demonstrated the most substantial renal recovery, achieving normal values for creatinine (Cr), blood urea nitrogen (BUN), eGFR, and uric acid (UA). Cr fell from 125.8 ± 15.6 μmol/L to 62.4 ± 6.9 μmol/L, BUN decreased to 4.8 ± 0.8 mmol/L, and UA dropped to 238 ± 30 μmol/L, all within healthy reference ranges. eGFR improved markedly to 90.2 ± 10.4 mL/min/1.73m^2.

CG achieved partial improvement, while OG showed minimal recovery.

These findings suggest that HU-PLGA-NPs not only correct hematologic abnormalities but also markedly protect renal function, reducing

[Downloaded from mail.ijrr.com on 2026-11-11]

[DOI: 10.61186/ijrr.24.4.10]

polycythemia-related renal stress and hydroxyurea toxicity.

DISCUSSION

Our findings suggest that HU delivered via PLGA nanoparticles improves the hemostatic milieu beyond what is typically expected from hematocrit reduction alone. The high-altitude literature shows that coagulation/fibrinolysis responses are heterogeneous: some models and populations demonstrate dynamic, time-dependent procoagulant/fibrinolytic derangements during hypoxic exposure/acclimatization, whereas other well-controlled field studies in Andean highlanders with excessive erythrocytosis do not consistently support a uniform "hypercoagulable" plasma profile and instead implicate platelet/whole-blood properties as important contributors [18]. This variability is consistent with the concept that thrombotic risk at altitude is shaped by interacting factors (hematocrit/viscosity, platelets, fibrin architecture, endothelium, hydration, comorbidities, and exposure pattern) rather than a single coagulation pathway abnormality [19].

Within this framework, your observation that treatment improved fibrinogen- and D-dimer–related patterns can be discussed as a likely downstream benefit of improved hemorheology/microvascular flow and reduced hypoxia-driven inflammatory signaling-mechanistically plausible and aligned with studies demonstrating that hypoxia exposure can modulate fibrinolytic parameters and coagulo-fibrinolytic dynamics [20].

Compared with the broader high-altitude and hemorheology literature, our pattern of improvements is consistent with the view that clinically meaningful benefit in excessive erythrocytosis requires more than simply lowering Hb/Hct: chronic mountain sickness/high-altitude polycythemia is strongly linked to impaired microcirculatory flow through increased viscosity, RBC aggregation, and altered RBC mechanical properties, which are recognized determinants of oxygen delivery at the capillary level [21]. In that context, the more complete correction of viscosity/ aggregation/deformability in the HU-PLGA-NP group is aligned with foundational work showing that hemorheology depends not only on hematocrit but also on RBC biomechanics and aggregation behavior (and these factors can dominate low-shear microvascular resistance) [22]. Additionally, recent characterization of RBC properties in chronic mountain sickness highlanders underscores that RBC "quality" metrics (including deformability/ biophysical features) are relevant to pathophysiology and potential interventions, supporting our interpretation that rheological improvements represent a mechanistic benefit rather than a purely descriptive change [23]. On the delivery side, the superior global profile we observed with nanoparticle HU is consistent with extensive evidence that PLGA systems can provide controlled release and altered biodistribution-often reducing peak-related off-target exposure-compared with free drug administration [21].

A strength of the study is its focus on hemorheological endpoints (viscosity, aggregation, deformability), because rheology is directly linked to oxygen delivery at the capillary level. Classic and contemporary hemorheology literature emphasizes that apparent blood viscosity is not driven solely by hematocrit; RBC aggregation and deformability substantially influence low-shear microvascular flow, and impaired deformability can exacerbate tissue hypoxia even when bulk oxygen content is high [24].

Recent work on red cell biomechanics in chronic mountain sickness further supports that RBC mechanical/biophysical properties are clinically meaningful in this setting. A study by Stauffer *et al.* [25] evaluated the biomechanical properties of RBCs from chronic mountain sickness patients and highlighted that RBC quality metrics such as deformability are relevant to physiology and potential clinical applications. This supports the rationale for interpreting your rheology improvements as a mechanistically important therapeutic effect rather than a purely descriptive laboratory change.

The more complete correction observed with HU-PLGA-NPs is consistent with established principles of PLGA-based delivery systems. PLGA is widely used because it is biocompatible/biodegradable and can enable controlled drug release and altered biodistribution, which may reduce peak-related off-target toxicity and improve exposure at intended sites [21]. In contrast, hydroxyurea-while clinically valuable-has a recognized toxicity profile (most notably myelosuppression, and broader systemic adverse effects depending on population and context). A concise, evidence-based way to frame safety is to acknowledge known toxicities while emphasizing that delivery strategies aimed at smoothing exposure can plausibly improve tolerability.

Several limitations of this study should be acknowledged. First, the work was conducted in a rat model of hypobaric hypoxia, which, although widely used, cannot fully reproduce the complexity of human high-altitude exposure, genetic adaptation, and environmental variability. Second, while the nanoparticles were radiolabeled, systematic in vivo imaging and quantitative biodistribution analyses were not comprehensively explored; future studies should directly correlate regional uptake with therapeutic efficacy. Third, the observation period was limited to 12 weeks, and long-term safety, cumulative toxicity, and potential immunogenic effects of repeated nanoparticle or radiotracer

[Downloaded from mail.ijrr.com on 2026-11-11]

[DOI: 10.61186/ijrr.24.4.10]

administration remain unknown. Finally, only a single nanoparticle formulation and dosing regimen were evaluated; optimization of polymer composition, surface functionalization, and radionuclide selection may further enhance targeting and imaging performance.

CONCLUSION

This study demonstrates that hydroxyurea-loaded PLGA nanoparticles significantly improve therapeutic outcomes in an experimental model of high-altitude polycythemia compared with conventional hydroxyurea. The nanoparticle platform effectively corrected hematologic, coagulation, and hemorheological abnormalities while providing better liver and kidney safety, likely through targeted and sustained drug delivery. These findings suggest that HU-PLGA-NPs represent a safer and more efficient therapeutic strategy for HAPC and provide a promising basis for future imaging-guided, individualized treatment approaches.

***Funding*:** This research did not receive any specific grant from funding agencies in the public, commercial, or not-for-profit sectors.

***Data availability*:** The datasets generated and/or analyzed during the current study are available from the corresponding author on reasonable request.

***Ethical compliance*:** All animal experiments described in this article were reviewed and approved by the Chengdu University of Traditional Chinese Medicine Laboratory Animal Welfare Ethics Committee (Approval No. 2023031) and were conducted in accordance with all relevant guidelines, regulations, and legal and ethical standards for the care and use of laboratory animals.

***Conflict of interest*:** The authors declare that they have no conflicts of interest related to this work.

***Authors contribution*:** J.N., Conceptualization, Methodology, Investigation, Data Curation, Formal Analysis, Writing - Original Draft, Writing - Review & Editing, Visualization. D.W., Methodology, Investigation, Data Curation, Writing - Review & Editing. M.J.L., Conceptualization, Supervision, Funding Acquisition, Writing - Review & Editing.

***AI usage*:** The authors confirm that no artificial intelligence (AI) tools were used in the generation or writing of this manuscript.

REFERENCES

1. Hancco I, Bailly S, Baillieul S, Doutreleau S, *et al.* (2020) Excessive erythrocytosis and chronic mountain sickness in dwellers of the highest City in the world. *Frontiers in Physiology, **11**: 773.*
2. Tang S, Zhou W, Chen L, Yan H, *et al.* (2024) High altitude polycythemia and its maladaptive mechanisms: an updated review. *Frontiers in Medicine, **11**: 1448654.*
3. Schmidt WFJ, Wachsmuth N, Jimenez J, Soria R (2022) Hemoglobin Mass and Blood Volume in Patients With Altitude-Related Polycythemia. *Frontiers in Physiology, **13**: 867108.*
4. Schmidt WFJ, Wachsmuth NB, Romero Pozo MC, Aguilar Valerio MT, *et al.* (2023) Possible strategies to reduce altitude-related excessive polycythemia. *J Appl Physiology, **134** (6): 1321-1331.*
5. Song Z, Zhang A, Luo J, Xiong G, *et al.* (2023) Prevalence of high-altitude polycythemia and hyperuricemia and risk factors for hyperuricemia in high-altitude immigrants. *High Altitude Medicine & Biology, **24** (2): 132-138.*
6. Wu W, Ni Y, Sun W, Zhou W, *et al.* (2026) Elevated red cell distribution width is an indicator for chronic mountain sickness in high altitude polycythemia patients: A retrospective study. *Respiratory Medicine, **251**: 108588.*
7. Yin R, Wu Y, Li M, Liu C, *et al.* (2024) Association between high-altitude polycythemia and hypertension: a cross-sectional study in adults at Tibetan ultrahigh altitudes. *Journal of Human Hypertension, **38**(7): 555-560.*
8. Adams E and Peel T (2025) Chronic Mountain Sickness: A comprehensive review of current management and proposals for novel therapies. *High Altitude Medicine & Biology, **26**(3): 318-327.*
9. Griesshammer M (2016) Hydroxyurea significantly increases skin toxicity in patients with MPN. *Leukemia Research, **44**: S8-S9.*
10. Ferrari A, Carobbio A, Masciulli A, Ghirardi A, *et al.* (2019) Clinical outcomes under hydroxyurea treatment in polycythemia vera: a systematic review and meta-analysis. *Haematologica, **104**(12): 2391-2399.*
11. Sharma S, Parmar A, Kori S, Sandhir R (2016) PLGA-based nanoparticles: A new paradigm in biomedical applications. *TrAC Trends in Analytical Chemistry, **80**: 30-40.*
12. Karwasra R, Bano N, Ahmad S, Singh S, *et al.* (2026) Multimodal evaluation of mannose engineered poly lactic glycolic acid nanoparticles with granulocyte colony stimulating factor focused delivery to bone marrow for neutropenia. *Scientific Reports, **16** (1): 2849.*
13. Cruz LJ, Rezaei S, Grosveld F, Philipsen S, Eich C (2022) Nanoparticles targeting hematopoietic stem and progenitor cells: Multimodal carriers for the treatment of hematological diseases. *Front Genome Ed, **4**: 1030285.*
14. Cruz LJ, van Dijk T, Vepris O, Li TMWY, *et al.* (2021) PLGA-nanoparticles for intracellular delivery of the crispr-complex to elevate fetal globin expression in erythroid cells. *Biomaterials, **268**: 120580.*
15. Pellico J, Gawne PJ, TM de Rosales R (2021) Radiolabelling of nanomaterials for medical imaging and therapy. *Chemical Society Reviews, **50**(5): 3355-3423.*
16. Gawne PJ, Man F, Blower PJ, TM de Rosales R (2022) Direct cell radiolabeling for *in vivo* cell tracking with PET and SPECT imaging. *Chemical Reviews, **122**(11): 10266-10318.*
17. Núñez-Salinas A, Parra-Garretón C, Acuña D, Peñaloza S, *et al.* (2025) Nanoradiopharmaceuticals: Design principles, radiolabeling strategies, and biomedicine applications. *Pharmaceutics, **17**: (7): 912.*
18. Champigneulle B, Caton F, Seyve L, Stauffer É, *et al.* (2024) Are coagulation profiles in Andean highlanders with excessive erythrocytosis favouring hypercoagulability? *Exp Physiol, **109**(6): 899-914.*
19. Zhong X, Ye Z, Zhou X, Jiang R, *et al.* (2022) Time Course of Coagulo-Fibrinolytic Derangements During Acclimatization to High Altitude in Rabbits and a Preliminary Study on the Possible Mechanisms. *High Alt Med Biol, **23**(3): 240-248.*
20. Jiang P, Wang Z, Yu X, Qin Y, *et al.* (2021) Effects of long-term high-altitude exposure on fibrinolytic system. *Hematology, **2**(1): 503-509.*
21. Makadia HK and Siegel SJ (2011) Poly lactic-co-glycolic acid (PLGA) as biodegradable controlled drug delivery carrier. *Polymers (Basel), **3** (3): 1377-1397.*
22. Williams A, Govender K, Cabrales P (2020) What determines blood viscosity at the highest city in the world? *The Journal of Physiology, **598**(18): 3817-3818.*
23. Stauffer E, Pichon AP, Champigneulle B, Furian M, *et al.* (2024) Making a virtue out of an evil: Are red blood cells from chronic mountain sickness patients eligible for transfusions? *American Journal of Hematology, **99**(7): 1407-1410.*
24. Baskurt OK and Meiselman HJ (2003) Blood rheology and hemodynamics. *Semin Thromb Hemost, **29**(5): 435-450.*
25. Stauffer E, Pichon AP, Champigneulle B, Furian M, *et al.* (2024) Making a virtue out of an evil: Are red blood cells from chronic mountain sickness patients eligible for transfusions? *Am J Hematol, **99**(7): 1407-1410.*

[Downloaded from mail.ijrr.com on 2026-11-11]

[DOI: 10.61186/ijrr.24.4.10]

[DOI: 10.61186/ijrr.24.4.10] [Downloaded from mail.ijrr.com on 2026-11-11]